AIP | Review of Scientific Instruments

Tangential soft x-ray camera for Large Helical Device

S. Ohdachi, K. Toi, G. Fuchs, and S. von Goeler

Citation: Rev. Sci. Instrum. **72**, 724 (2001); doi: 10.1063/1.1324741

View online: http://dx.doi.org/10.1063/1.1324741

View Table of Contents: http://rsi.aip.org/resource/1/RSINAK/v72/i1

Published by the American Institute of Physics.

Tangential soft x-ray camera for Large Helical Device

S. Ohdachi[a] and K. Toi
National Institute for Fusion Science, Toki 509-5292, Japan

G. Fuchs
Institut für Plasmaphysik, Forschungszentrum Jülich GmbH, EURATOM Association, D-52425 Jülich, Germany

S. von Goeler
Princeton Plasma Physics Laboratory, Box 451, Princeton, New Jersey 08543

(Presented on 20 June 2000)

A tangentially viewing soft x-ray camera system is to be installed on the Large Helical Device (LHD). This camera system is aimed at exploring both detailed structures of the magnetic surfaces of the LHD plasma and helical islands induced either due to magnetic field errors or MHD instabilities. The frequency range this system is capable of exploring is $0<v<2$ kHz; this range can be extended, if the space resolution or the viewing area were reduced. © *2001 American Institute of Physics.* [DOI: 10.1063/1.1324741]

I. INTRODUCTION

A tangentially viewing camera can provide pictures with good spatial resolution. The pictures can then be used to infer the shape of the flux surfaces as well as disturbances due to both field errors and MHD activities. The retrieval of the shape of the flux surfaces in a helical system is more complicated as compared to that in tokamaks where the cross section of the flux surface in the poloidal planes is just the same at any toroidal angle. In an helical system, the toroidal magnetic field component is much larger than the other components; for this reason, a toroidally viewing camera does give advantages due to the fact that the emission can be expected to be constant along fieldlines.[1,2]

Steep temperature gradients in the boundary area have been found in LHD (Large Helical Devices, a heliotron/torsatron type device with $R/\overline{a}=3.9/0.6\,\mathrm{m}$),[3] which are so far not fully explained by theory. When the heating power is further increased, MHD instabilities might be strongly destabilized in the plasma boundary of LHD. Note that, in heliotron/torsatron type devices, such as LHD, the rotational transform $i/2\pi$ does increase toward the boundary and can be close to 1 there. Therefore, several low-order rational surfaces, $i/2\pi=1$, 1/2, 2/3 and so on, do exist inside the plasma of LHD. We are planning to install a tangentially viewing soft x-ray camera in LHD to detect MHD instabilities excited near the rational surfaces.

A tangentially viewing soft x-ray camera (TSXC) has been developed in a collaboration with the National Institute for Fusion Science, Japan (NIFS), Princeton Plasma Physics Laboratory (PPPL), and the Institut für Plasmaphysik Jülick, Germany (IPP), and has been used on TEXTOR-94 Tokamak since 1998.[4] After the experiments on TEXTOR-94, in 2000, this system will be installed in LHD in order to test the applicability to a no-tokamak plasma. The design of TSXC for the LHD device is described in Sec. II with the emphasis on some improvements—a new charge-coupled device (CCD) camera and a filter exchange mechanism—to the present camera. An analyzing method of the images obtained with the camera in LHD is described in Sec. III. The possibility that the island structure can be derived from the images is discussed there as well.

II. EXPERIMENTAL SETUP

The setup of the camera system is shown in Fig. 1. It is similar to that described in Ref. 2, as it first converts the x-ray photons to visible light, using a large scintillator plate. This does give advantages for the time resolution as compared to direct conversion; however, at the expense that it is also more complicated (cf. Ref. 2). For the 7 windows we use beryllium foils with thickness ranging from 8 to 80 μm, together with 7 pinholes from 1 to 5 mm; they are all on one rod and can be exchanged using an ultrasonic motor. A 9 m long optical fiber bundle is used to guide the visible light away from the area with a strong magnetic field. The light is amplified using a Hamamatsu V4440U-mod electron beam imaging amplifier, where the image is reduced to 25 mm diam. The image is further reduced to 9 mm diam by a taper and is intensified by a multichannel type amplifier which is also used as a fast electrical shutter (>10 ns). Finally, the amplified image is stored with a fast framing CCD camera,

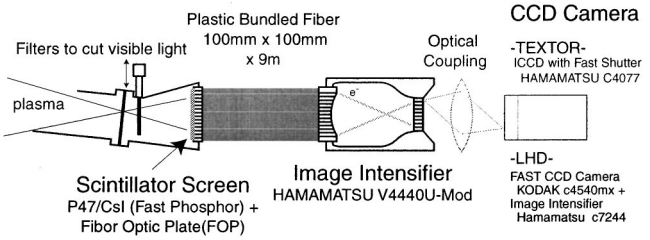

FIG. 1. Basic arrangement of the tangential SX camera.

[a]Electronic mail: ohdachi@nifs.ac.jp

TABLE I. Specifications of CCDs. The new CCD will be tested in LHD.

Model No.	Resolution	D/A	Exposure time	Framing interval	Storage
C4077	350				
Hamamatsu	lines	Analog	1 μs~16 ms	1/60 s	8
4540 mx	256×256	digital 8 bit	50 ns~10 ms	1/30−1/4500 full frame	8192
Kodak		with external I.I. unit	1/9000–1/4500 part frame		

Kodak C4540MX. The resolution of this camera is 256×256 pixels; the camera is normally operated with a framing rate up to 4 kHz. The framing rate can be enhanced up to 40 kHz by reducing the number of pixels used. The data are first stored in the camera memory (512 Mbyte) and later on collected in a windows NT based PC system. The difference in the specification of the old/new CCD camera are summarized in Table I.

The distance from the plasma to the scintillator screen is about twice as long as that in TEXTOR-94. From geometrical considerations in LHD, the number of photons which enter in a ''PIXEL'' on the phosphor screen (1×1 mm) is about 10^7 s^{-1}, assuming that the electron temperature at the center $T_{e0}=2$ keV, the line averaged electron density $n_e=2\times10^{19}$ m^{-3}, the effective ion charge $Z_{\text{eff}}=1$, the aperture diameter of the pinhole $a_p=1$ mm, and the cutoff energy of the filter $E_c=1.3$ keV (corresponds to 15 μm beryllium foil). A triangular shape of the electron temperature profile and a flat density profile are thereby assumed. The ratio of the numbers of the injected photons (with an energy 1.5 keV) to the photoelectrons at the entrance of the intensifier tube is estimated by 1 to 0.16.[2] Statistics of the photon number at the entrance of the intensifier tube determines the noise level. When the camera is operated with a framing rate of 1 kHz, the relative noise due to the photon counting process is about 8%. Measurements are marginally possible under this condition. However, as this estimate is the most pessimistic one (e.g., $Z_{\text{eff}}=1$), we can anticipate enhanced SX emission for a plasma in the next experimental campaign with larger heating capability.

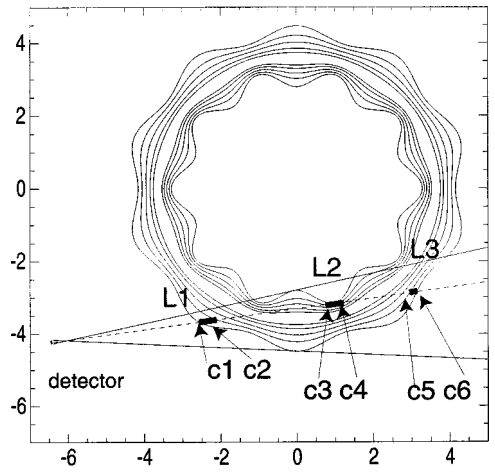

FIG. 2. Sightlines of TSXC and magnetic surfaces in LHD.

III. ESTIMATION OF IMAGE

Here we discuss the feasibility of fluctuation measurements on LHD. We do this by calculating the images to be expected for different plasmas with plausible profiles of T_e and n_e. We do have a three-dimensional object and we can with one camera only obtain a two-dimensional image of it. Unless we put on a constraint, we cannot retrieve the object from that image. Therefore we assume the local emission to be constant along the magnetic flux lines. The image is the radon transformed (see Deans[5]) of the object. For a finite set of pixels P_{ij} making up the image, this projection can be expressed in matrix form

$$P=RI, \tag{1}$$

with R the projection matrix and I the local emission. The elements of R are to be derived from the geometry, namely by the length of the elements of the line of sight in between subsequent flux surfaces.

Whereas the calculation of R_{ij} is rather easy in a tokamak case, the shape of the LHD plasma is not simple. The magnetic surface is predicted by an MHD equilibrium code VMEC. The shape is represented by a superposition of many toroidal and poloidal Fourier modes (typically 90) and can

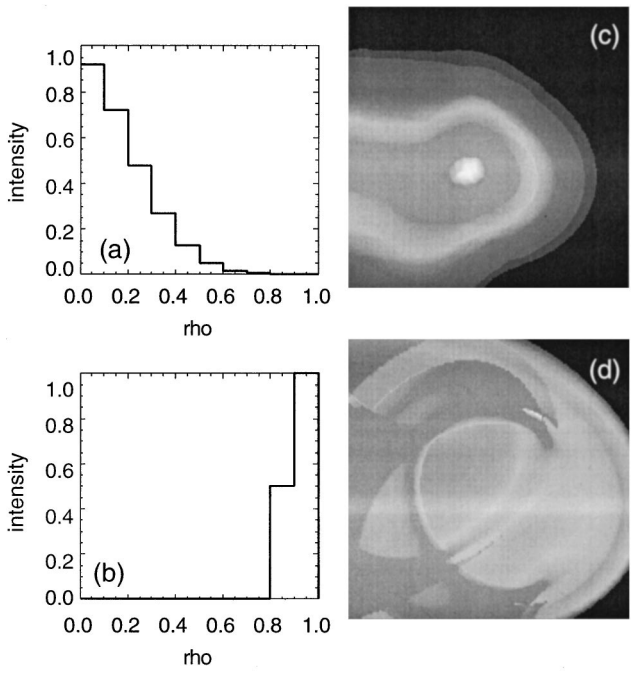

FIG. 3. Simulated images of TSXC [(c) and (d)] for the LHD configuration assuming peaked (a) and very hollow (b) emissivity profiles, respectively.

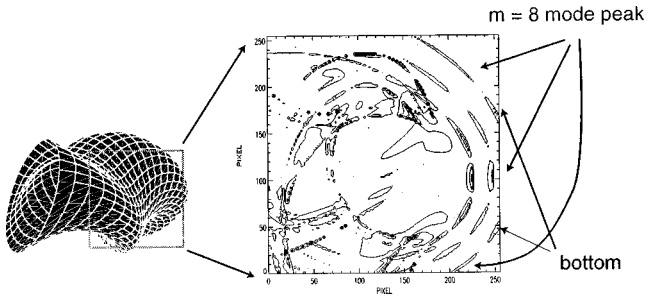

FIG. 4. Contour map of the image with $m/n=8/8$ helical island deformation of the magnetic surface. The outer shape of the LHD plasma is also shown for reference.

not be expressed analytically. We therefore approximate the shape by 261 120 triangular planes. That is, the magnetic surface is divided by 64 in poloidal, 204 in toroidal, and 10 layer and each plane is divided into two triangles in this simulation. Determination of the positions of intersections ($c1, c2$,..., in Fig. 2) between magnetic surfaces and a sightline becomes much easier, though it takes a lot computation time. Once we determine the matrix elements R_{ij}, the calculation for various emission profiles can easily be done. Examples of the calculated images with different emissivity profiles are shown in Fig. 3. This type of matrix representation is convenient not only for the prediction. If Eq. (1) can be solved for I with given experimental data, we can determine the local emissivity on each flux surface. As the tomographic problem is known to be ill-posed[5] we might need some kind of elaborate numerical technique to obtain stable solutions.[6]

Another interesting application of this method is to test the possibility of measuring magnetic islands. Since the magnetic surfaces are now represented by polygons, it is easy to project island structure by deforming the shape of the magnetic surfaces. We try to simulate islands of the $\iota/2\pi=1$ rational surface. Indeed, in LHD, MHD instabilities with the mode numbers of $m/n=2/2$, 3/3 have been observed experimentally.[7–9] The image with $m/n=8/8$ islands at the $\iota/\pi=1$ ($\rho\sim0.9$) surface is shown in Fig. 4. This image has been obtained by taking the difference between a reference image with no island deformation and such a one with deformation. The $m=8$ island can be observed at the outboard side of the plasma, where the sightlines penetrate the plasma once only, and are almost parallel to the magnetic field lines.

There will be no reference image of this type in the real experiments. However, the reference image can be made by averaging over many frames if the island structure rotates in toroidal and poloidal directions. The time evolution of the island can be seen by calculating the difference between each temporal frame and the reference image.

IV. CONCLUSION

Implementation of TSXC on LHD has been discussed. The simulation of the images demonstrated the expected performance of TSXC. The camera system is capable of measuring magnetic island even in heliotron/torsatron configurations. The TSXC on LHD will be put in operation in the next experimental campaign of LHD (from September 2000 to March 2001).

[1] S. von Goeler *et al.*, Rev. Sci. Instrum. **65**, 1621 (1994).
[2] S. von Goeler *et al.*, Rev. Sci. Instrum. **70**, 602 (1999).
[3] N. Ohyabu *et al.*, Phys. Rev. Lett. **84**, 103 (2000).
[4] G. Fuchs *et al.*, in *Controlled Fusion and Plasma Physics*, Proceedings of 26th EPS Conference, Madstricht, 1999, ECA Vol. 23J, p. 757.
[5] S. R. Deans, *The Radon Transform and Some of its Applications* (Wiley, New York, 1983).
[6] V. Pickalov and G. Fuchs, in *Controlled Fusion and Plasma Physics*, Proceedings of 27th EPS Conference, Budapest (to be published).
[7] M. Takechi *et al.*, J. Plasma Fusion Res. (in press).
[8] S. Ohdachi *et al.*, Rev. Sci. Instrum. (these proceedings).
[9] K. Toi *et al.*, in *Controlled Fusion and Plasma Physics*, Proceedings of 27th EPS Conference, Budapest (to be published).